Polymer 50 (2009) 6172–6185

Contents lists available at ScienceDirect

Polymer

journal homepage: www.elsevier.com/locate/polymer

Theoretical investigation on the white-light emission from a single-polymer system with simultaneous blue and orange emission

Bo Hu [a,b], Jingping Zhang [a,*]

[a] Faculty of Chemistry, Northeast Normal University, Changchun 130024, China
[b] Faculty of Chemistry, Jilin Normal University, Siping 136000, China

ARTICLE INFO

Article history:
Received 8 September 2009
Received in revised form
13 October 2009
Accepted 13 October 2009
Available online 17 October 2009

Keywords:
WPLEDs
Electronic and optical properties
Reorganization energy

ABSTRACT

White organic light-emitting devices (WOLEDs) have attracted considerable attention because of their good potential for various lighting applications. Among these devices, WOLEDs based on polymers (WPLEDs) are of particular interest. We report here a theoretical investigation of the white-light emission from a single-polymer system with simultaneous blue (polyfluorene as a blue host) and orange (2,1,3-benzothiadiazole-based derivative as an orange dopant) emission. A variety of theoretical methods are used and evaluated to calculate electronic and optical properties of polyfluorene and 2,1,3-benzothiadiazole-based derivatives. Simulated electronic and optical properties are found to agree well with available experimental measurements. The influence of the "CH"/N heterosubstitution on the electronic and optical properties of the 2,1,3-benzothiadiazole-based derivative is considered. Furthermore, we find that the electronic and optical properties of "CH"/N substitution derivatives can be tuned by symmetrically adding suitable electron-donating groups on *N*,*N*-disubstituted amino groups, implying good candidates as orange dopants in WPLEDs with polyfluorene as a blue-light-emitting host. Solvent (dichloromethane) effects on the electronic and optical properties of 2,1,3-benzothiadiazole-based derivatives have been investigated. In addition, low reorganization energy values of holes for designed 2,1,3-benzothiadiazole-based derivatives within the framework of the charge hopping model suggest them to be good hole transfer materials.

© 2009 Elsevier Ltd. All rights reserved.

1. Introduction

White organic light-emitting devices (WOLEDs) have received great attention due to their good potential lighting applications in low-cost backlighting in liquid–crystal displays, in full-colour displays, and as next-generation lighting sources envisioned to replace the incandescent light bulb and fluorescent lamp [1–23]. Among these devices, WOLEDs based on polymers (WPLEDs) are of particular interest because they can be easily fabricated using wet processes, including the spin casting, screen-printing, and ink-jet printing techniques, which are expected to be lower in cost in mass production, especially in the production of large-area panel displays [15–23]. Several approaches including polymer blends [15], polymer doped with dyes [16], bilayer exciplex [17], and single-polymer with different functional groups [18–23] have been reported for achieving efficient WPLEDs. However, WPLEDs fabricated with polymer-blend or small-molecule-doped polymer systems have great disadvantages, for example, it is difficult to control the doping level of the long wavelength light-emitting materials and, thus, to obtain balanced white-light emission, as well as low electroluminescence (EL) efficiency, and spectral dependence on the applied voltage. White EL from a single-polymer is extremely desirable because it can offer several distinct advantages, such as low cost, simple fabrication processes, and ease of scaling up, without any problems associated with phase separation of components.

In the past few years, therefore, how to generate highly efficient, stable, and pure-white-light-emitting devices from a single-polymer has attracted growing interest and the encouraging progress has been made [18–23]. In this field, Wang et al. propose a novel strategy to realize the white EL with simultaneous blue, green, and red emission from a single-polymer [18]. This is achieved by attaching a small amount of a green-emissive component to the pendant chain and incorporating a small amount of a red-emissive component into the main chain of the macromolecule, which itself has a blue emission. Similarly, they also propose a strategy to develop the white emission from a single-polymer by incorporating a small amount of orange emission component into a blue-light-

* Corresponding author. Fax: +86 431 85099521.
E-mail address: zhangjingping66@yahoo.com.cn (J. Zhang).

0032-3861/$ – see front matter © 2009 Elsevier Ltd. All rights reserved.
doi:10.1016/j.polymer.2009.10.034

emitting polymer [19]. For example, they succeed in realizing highly efficient white EL with simultaneous blue and orange emission from a single-polymer, in which a small amount of orange-light-emissive 1,8-naphthalimide derivatives or 2,1,3-benzothiadiazole (BTD) derivatives are incorporated into the main chain of a blue-light-emitting polyfluorene.

In parallel to recent experimental work on the WPLEDs, theoretical efforts have indeed begun to constitute an important source of valuable information, complementing the experimental studies in the characterization of the nature and the properties of the ground-states and lowest electronic excited states. A number of studies demonstrate the interplay between theory and experiment, which is capable of providing useful insights to the understanding of the molecular electronic structure of the ground and excited state as well as the nature of absorption and photoluminescence [24–30]. The aim of this article is to provide an in-depth interpretation of the available experimental electronic and spectroscopic characteristics reported for the single-polymer system using theoretical approaches. Furthermore, quantum-chemical studies of the substitution effect on the electronic and optical properties of BTD-based derivatives are thereby called for designing novel functional materials.

The first part of this paper, therefore, we select single-polymer electroluminescent system containing two individual emission species (polyfluorene, PF_n, as a blue host and a BTD-based derivative, $(OMC\text{-}CH_3)_m$, as an orange dopant) [19c] as model compounds (shown in Fig. 1a) to explore their experimentally observed electronic and spectroscopic behaviors in depth on the basis of the quantum-chemical calculations. In the second part, the influence of the "CH"/N heterosubstitution on the electronic and optical properties of the BTD-based derivative (OMC, shown in Fig. 1b) is considered. OMC, so-called donor–π-bridge–acceptor–π-bridge–donor (D–π–A–π–D)-type molecule, is designed on the basis of a combination of the BTD moiety and two terminal electron-donating amino groups by benzene spacer. Lin, Tao and coworkers [31a] have shown that donor(D)–acceptor(A) molecules featuring benzothiadiazole and amino groups are attractive candidates for electro-optic applications. Their architecture, including the low-bandgap core and suitably substituted peripheral functional groups, leads to molecules with tunable emission characteristics, enhanced hole/electron affinity, and promising thermal characteristics. Mataka and coworkers [31b] have demonstrated that a series of D – π–A – π–D-type BTD-based dyes possessing terminal *N*,*N*-disubstituted amino groups provide high fluorescence quantum yields among the orange-red colour region as well as large two-photon absorption cross-sections in the near IR region. As far as we know, "CH"/N substitution approach, which has been cited as an efficient approach for tuning of the emitting colour in the case of Mq_3 (M = Al [25h,32,33], Ga [25h,32] and q = 8-hydroxyquinoline) based fluorescent materials, has not been exploited yet in the case of BTD-based materials. Therefore, in this contribution, as a systematic study, we take OMC as parent compound to investigate the effect of the "CH"/N substitution of spacer on their electronic and optical properties. OMC has been chosen because of the existence of X-ray crystallographic data and experimental absorption and fluorescence spectra, allowing thus a direct comparison between experimental and calculated results. The calculated values are compared with the available experimental data to test the theoretical methods. OMC is theoretically analyzed and used as referential systems to perform structural modifications in order to develop new systems. In the third part, we find that the electronic and optical properties of "CH"/N substitution derivatives can be modulated by symmetrically adding electron-donating groups [$-CH_3$, $-OCH_3$, $-NH_2$, and $-N(CH_3)_2$] on *N*,*N*-disubstituted amino groups (shown in Fig. 1b), implying a potential application as orange dopants in WPLEDs with PF_n as a blue-light-emitting host. Finally, a discussion on the reorganization energies of BTD-based derivatives has been carried out to investigate the charge carrier properties of designed compounds. To the best of our knowledge, no detail theoretical investigation for designed compounds has been performed to date. A detailed knowledge of these issues is essential for the understanding of WPLEDs operation and for the design of novel advanced materials.

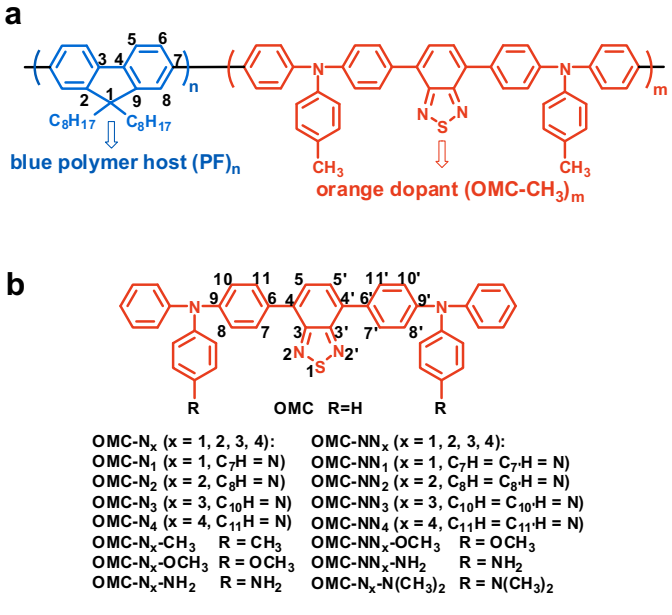

Fig. 1. (a) The chemical structure of the model polymer —$(PF)_n$—$(OMC\text{-}CH_3)_m$—. (b) Chemical structures of the investigated BTD-based derivatives (OMC and its derivatives).

2. Computational details

We take OMC as the reference sample to compare the performance of various methods. The 6-31G(d) [34–36] split valence polarized basis set is employed through out. This basis set has been tested extensively and has been shown to yield reliable results for geometries and excited state of the organic light-emitting materials [30]. The corresponding results as well as the available experimental data [31] are listed in Tables S1–S2 (in the Supporting Information) for comparison.

The S_0 geometry of OMC is optimized in the gas phase using ab initio Hartree–Fork (HF) [37] and density functional theory (DFT) [38] with the hybrid functional methods (B3LYP [39,40,41a], B3P86 [41–43], B3PW91 [41a,42–44], PBE0 [45]). Geometry optimizations are restricted to C_2 symmetry. To compare the optimized results with the experimental data, Table S1 (in the Supporting Information) collects the selected bond lengths, bond angles, and dihedral angles in the optimized S_0 geometries, as well as the corresponding X-ray data [31]. From a careful analysis of the optimization results, a good agreement can be observed between our results and experimental data [31], except for the parameters involving N_2–C_3 of 1.301 Å by HF and S_1–N_2 of 1.642 Å by B3LYP, whose deviation from the experimental values [31] (1.349 and 1.609 Å) is 0.048 and 0.033 Å. On the basis of the optimized S_0 geometries, the visible absorption spectra, or more specifically the maximum (one-photon) absorption wavelength (λ_{abs}) are obtained respectively using time-dependent DFT (TD–DFT) [46–48] with B3LYP, B3P86, B3PW91, and PBE0 functionals. From the results listed in Table S2 (in the Supporting Information), one may find that λ_{abs} (471.2 nm)

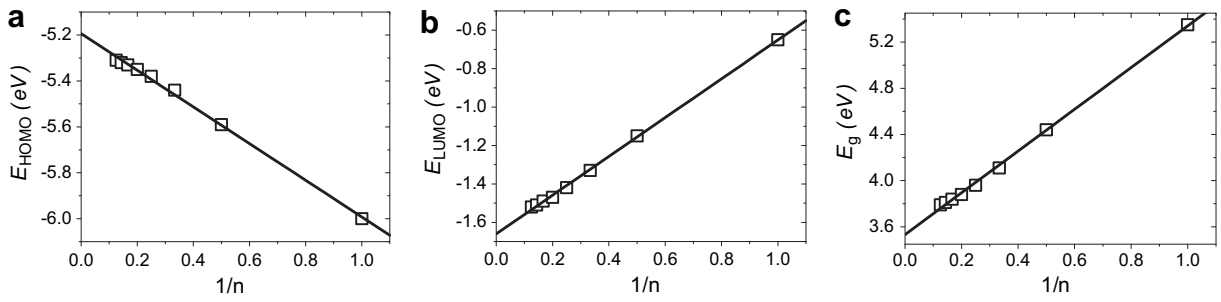

Fig. 2. (a) E_{HOMO}; (b) E_{LUMO}; (c) E_g as a function of reciprocal length n in oligomers of PF_n.

obtained at the TD-PBE0/6-31G(d)//HF/6-31G(d) level is quite close to the experimental value (459 nm) [31], with the deviation being 12.2 nm. Therefore, the absorption spectrum is calculated using TD-PBE0 with 6-31G(d) basis set based on the HF/6-31G(d) optimized S_0 geometries. PBE0/6-31G(d) single point energy calculations are performed to study the electronic properties in S_0. Studies of the excited-state properties for a number of molecules using the single configuration interaction (CIS) [49a] method have shown that, despite the tendency of CIS to overestimate electronic transition energies, the excited-state potential energy surface can often be quite accurate, as evidenced by comparison of equilibrium excited-state structure with experiments [49b–e]. The S_1 geometry is optimized at the CIS level along with 6-31G(d) basis set. The maximum emission wavelength ($\lambda_{em} = 617.1$ nm) calculated at TD-PBE0/6-31G(d)//CIS/6-31G(d) level is close to the experimental value (639 nm) [31] with the deviation being 21.9 nm, so TD-PBE0 functional in conjunction with 6-31G(d) basis set is appropriate to get the relatively reliable predictions on the emission spectrum. To explicitly take into account the solvent effects on the electronic and optical properties of the BTD-based derivatives, we adapt the self-consistent reaction field (SCRF) approach with the polarizable continuum model (PCM) [50] using CH_2Cl_2 solvent to calculate the electronic properties, absorption, and emission spectra. In addition, the reorganization energies of BTD-based derivatives are predicted from the single point energy at the B3LYP/6-31G(d,p) [34–36] level based on the PBE0/6-31G(d) optimized neutral, cationic, and anionic geometries.

Since the optoelectronic properties of conjugated oligomers converge rapidly with increasing chain size, we have considered oligomers PF_n containing from one to eight ($n = 1$–8) repeat units (shown in Fig. 1a). In the calculation, the alkyl chains (attached to the conjugated backbone to improve solubility) are systematically replaced by methyl groups since this does not affect the electronic and optical properties of the oligomers but significantly reduces calculation times. The S_0 geometry optimizations of PF_n with $n = 1$–8 are performed at the B3LYP/6-31G(d) level and C_2 symmetry constrains. Table S3 (in the Supporting Information) collects the selected bond lengths, bond angles, and dihedral angles in the optimized S_0 geometries, as well as available theoretical data [51]. It can be found that, our computational results are in good agreement with available theoretical data [51], the largest deviation being found to be about 1.56° for C_2–C_1–C_9. On the basis of the optimized S_0 geometries, electronic properties are calculated using PBE0 functional with 6-31G(d) basis set. Due to the large size of the PF_n ($n > 4$), it is difficult/impossible to succeed in the corresponding S_1 geometry optimization, owing to the computational limitations. Therefore, S_1 geometries consisting of one to four monomer units (PF_1–PF_4) have been optimized using CIS method. On the basis of the optimized S_0 and S_1 geometries, the electronic absorption and emission spectra are computed at the TD-PBE0/6-31G(d) level of theory, respectively.

All calculations in this work are carried out using Gaussian 03 package [52].

3. Results and discussion

3.1. Theoretical simulation and explanation for PF_n and OMC-CH_3

3.1.1. Electronic properties

A novel strategy to achieving white EL is to develop single-polymer systems with different emission components based on the control of energy transfer and charge trapping between the chromophores in the designed polymers [18,19]. In experiment, the highest occupied molecular orbital (HOMO) and lowest unoccupied molecular orbital (LUMO) energy levels of OMC-CH_3 lie between those of PF_n, indicating that charge trapping of the orange dopant unit is energetically favorable in the EL process. We have calculated the energies of the HOMO (E_{HOMO}), LUMO (E_{LUMO}), and the energy gaps E_g ($E_g = E_{LUMO}$-E_{HOMO}) for PF_n ($n = 1$–8) and OMC-CH_3 respectively, the corresponding values being listed in Tables S4 and S5 (in the Supporting Information).

E_{HOMO}, E_{LUMO}, and E_g for PF_n are plotted against the inverse number of repeat units in Fig. 2. A good linear relationship is found. The extrapolated E_{HOMO}, E_{LUMO}, and E_g to the infinite chain length are −5.19, −1.66, and 3.53 eV, respectively. The HOMO and LUMO energy levels of the OMC-CH_3 lie at −5.07 and −1.92 eV, respectively, and an E_g of 3.15 eV is obtained (see Table S5, the Supporting Information). In experiment, the HOMO and LUMO energies are estimated from the formulae based on the onset oxidation and reduction potentials. Although there are some deviations between the experimental data [19c] (E_{HOMO} and E_{LUMO}: −5.80 and −2.12 eV for PF_n, −5.25 and −3.06 eV for OMC-CH_3) and calculated results with respect to the HOMO and LUMO energies, they have the same

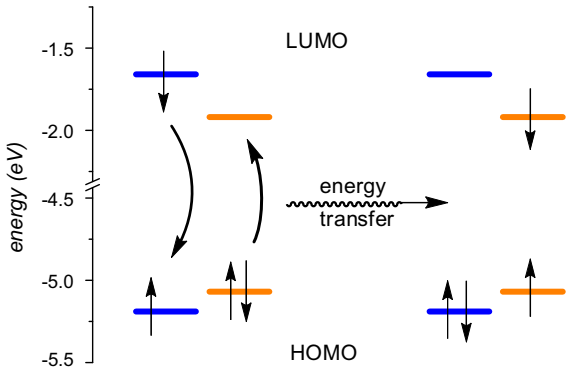

Fig. 3. Scheme of frontier molecular orbital levels for typical energy transfer in WOLED. Blue: polymer host (PF_n); Orange: dopant (OMC-CH_3). [For interpretation of the references to colour in this figure legend, the reader is referred to the web version of this article.]

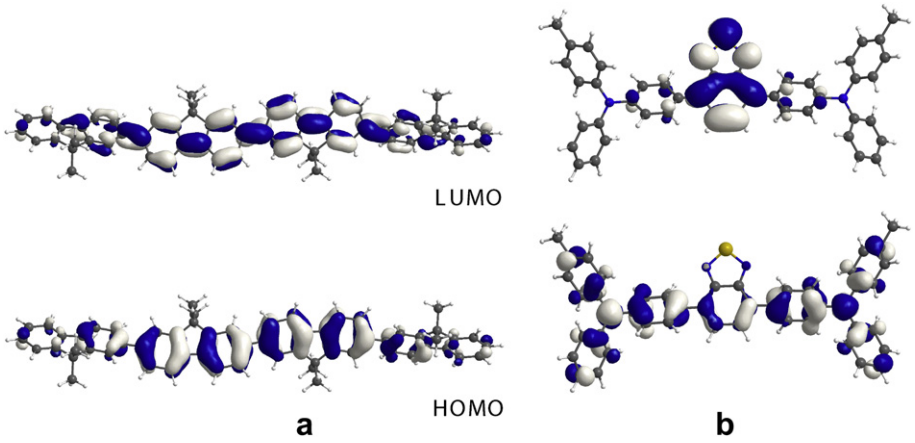

Fig. 4. HOMO and LUMO of (a) PF_4; (b) OMC-CH_3.

trend. As shown in Fig. 3, the HOMO and LUMO energy levels of OMC-CH_3 lie between those of PF_n, indicating that the energy transfer from PF_n to OMC-CH_3 is energetically favorable, which is in good accord with the experimental findings [19c].

Other than the E_{HOMO}, E_{LUMO}, and E_g values, another way to understand the electron transport in molecular devices is to analyze the shape of the frontier molecular orbitals (FMOs). From the FMOs in Fig. 4, the electronic density distribution is investigated. For PF_4, there is antibonding between the bridge atoms of the inter-ring, and there is bonding between the bridge carbon atom and its conjoint atoms of the intra-ring in the HOMO. On the contrary, there is bonding in the bridge single bond of the inter-ring and the antibonding between the bridge atom and its neighbor of the intra-ring in the LUMO. In the case of the OMC-CH_3, the electron density of HOMO is mainly localized on both triphenylamine units and that of LUMO mostly on the central BTD unit. This clearly indicates that this molecule possesses strong intramolecular charge transfer from the amino groups (donor) to BTD ring (acceptor) unit.

3.1.2. Optical properties

Wang et al. expect to realize individual emission from two emissive species — PF_n as a blue host and $(OMC\text{-}CH_3)_m$ as an orange dopant — for generating white emission with simultaneous emission from two colours [19c]. Incorporation of orange dopant unit results in an additional emission peak in the photoluminescence (PL) spectra. This is due to Förster energy transfer from the polymer backbone to the orange dopant unit because of the overlap of the absorption spectrum of OMC-CH_3 and the emission spectrum of PF_n. The vertical excitation energies, $\lambda_{abs}/\lambda_{em}$ and oscillator strengths for PF_n and OMC-CH_3 have been calculated and listed in Tables 1 and 2 respectively, together with other available experimental [53] and theoretical data [51].

Inspection of the TD–DFT results shows that, for both PF_n and OMC-CH_3, the transition in the absorption corresponds to the promotion of an electron from the HOMO to LUMO. While the emission is regarded as an electron transition process that is the reverse of the absorption, which corresponds to an electron transition configuration: LUMO → HOMO. Feng and coworkers [51] have calculated the electronic spectra of the PF_n by the ZINDO and TD-B3LYP methods. From these results listed in Table 1, a sufficiently good agreement can be observed between our results and available theoretical [51] and experimental data [53]. The λ_{abs} (from 263.1 to 387.9 nm) and λ_{em} (from 293.6 to 421.6 nm) of the PF_n increase with the extension of oligomers chain considerably. For the OMC-CH_3, the λ_{abs} and λ_{em} are calculated at 477.4 and 623.3 nm, respectively. Experimentally, Wang et al. [19c] design and synthesize single-polymer electroluminescent system containing two individual emission species — PF_n as a blue host and $(OMC\text{-}CH_3)_m$ as an orange dopant on the main chain. The resulting single-polymers are found to have highly efficient white EL with simultaneous blue and orange emission from the corresponding emitting species. Because of the large size of the studied polymer, the corresponding S_0/S_1 structure optimization is quite difficult in calculation. Therefore, the oligomer formed by two sections (PF_4 and OMC-CH_3) connected by four benzene rings, is introduced for calculation. The calculated emission spectrum of the oligomer is depicted in Fig. 5a. The emission spectrum shows dominant blue emission (424.9 nm) from the PF_4 and additional orange emission (625.6 nm) from the OMC-CH_3. Additional orange emission peak in the emission spectrum is due to the Förster energy transfer from the PF_4 to the OMC-CH_3 because of the overlap of the absorption spectrum of the OMC-CH_3 and the emission spectrum of PF_4 (PF_4 taken as reference in this work, the results can reflect the variation trend), as shown in Fig. 5b. Our calculation is in good agreement with the experimental findings [19c]. This may justify the choice of the methods and basis set used to calculate the electronic and optical properties for the molecules explored in this work.

3.2. "CH"/N substituted derivatives for OMC

With the aim to evaluate the influence of the "CH"/N heterosubstitution on the electronic and optical properties of the OMC,

Table 1
Optical properties of PF_n computed at the TD-PBE0/6-31G(d) level.

	Cal			Ref[a]		Exp[b]	
	E_v	λ	f	λ(ZINDO)	λ(TD-B3LYP)	ν_{abs}	λ
Absorption Properties							
$n=1$	4.71	263.1	0.29	247.9	260.8		
$n=2$	3.86	321.5	1.34	325.8	320.4	30400	328.9
$n=3$	3.53	351.7	2.21	346.7	354.2	28650	349.0
$n=4$	3.37	367.4	3.06	357.1	368.9	27550	363.0
$n=5$	3.30	376.3	3.92			27030	370.0
$n=6$	3.25	381.6	4.81	364.2	384.8	26880	372.0
$n=7$	3.22	384.9	5.72			26810	373.0
$n=8$	3.20	387.9	6.61	369.3	391.1		
Emission Properties							
$n=1$	4.22	293.6	0.43				
$n=2$	3.27	379.4	1.56	374.4	374.3	25770	388.0
$n=3$	3.03	408.8	2.44			23870	418.9
$n=4$	2.94	421.6	3.13	410.5	433.5	23200	431.0

[a] Reference data from Ref. [51].
[b] Experimental data from Re.f [53]. E_v = the vertical excitation energies (in eV). ν_{abs} = wavenumber (in cm^{-1}). λ = the maximum absorption/emission wavelength (in nm). f = the oscillator strength.

Table 2
Optical properties of OMC, OMC-CH_3, OMC-N_x, and OMC-NN_x ($x = 1$–4) computed at the TD-PBE0/6-31G(d) level.

	Absorption Properties						Emission Properties					
	Gas			CH_2Cl_2			Gas			CH_2Cl_2		
	E_v	λ_{abs}	f	E_v	λ_{abs}	f	E_v	λ_{em}	f	E_v	λ_{em}	f
Pristine												
OMC	2.63	471.2	0.44	2.57	483.1	0.47	2.01	617.1	0.79	1.90	651.4	0.90
OMC-CH_3	2.60	477.4	0.45	2.53	489.9	0.48	1.99	623.3	0.81	1.88	657.9	0.90
OMC-N_x												
OMC-N_1	2.76	449.0	0.38	2.65	468.4	0.39	2.17	570.3	0.95	2.01	616.0	1.01
OMC-N_2	2.66	465.3	0.44	2.60	476.4	0.46	2.04	607.5	0.78	1.95	636.8	0.87
OMC-N_3	2.65	467.3	0.42	2.60	476.9	0.44	2.02	614.4	0.75	1.93	641.2	0.86
OMC-N_4	2.58	480.6	0.51	2.49	497.4	0.57	2.03	609.7	0.83	1.91	647.6	0.95
OMC-NN_x												
OMC-NN_1	2.97	417.8	0.35	2.78	445.6	0.33	2.30	539.4	1.11	2.09	593.3	1.13
OMC-NN_2	2.73	454.6	0.51	2.69	460.8	0.56	2.08	595.5	0.77	2.01	617.6	0.86
OMC-NN_3	2.71	456.8	0.48	2.69	460.2	0.54	2.04	609.1	0.72	1.98	626.0	0.84
OMC-NN_4	2.58	480.3	0.66	2.46	503.6	0.74	2.06	602.6	0.84	1.93	643.7	0.98

E_v = the vertical excitation energies (in eV). $\lambda_{abs}/\lambda_{em}$ = the maximum absorption/emission wavelength (in nm). f = the oscillator strength.

both asymmetric OMC-N_x and symmetric OMC-NN_x ($x = 1$–4) substitutions are considered for this issue. The molecular models used in our calculations, obtained by a systematic substitution of CH groups with N atoms in positions 7, 8, 10, and 11 on the spacer benzene ring (see labeling scheme) for OMC-N_x ($x = 1$–4) on one hand, for OMC-NN_x ($x = 1$–4) on the other hand are shown in Fig. 1b. In the following, the results are presented according to the labeling way adopted in the same Figure.

3.2.1. Electronic properties

In Table S5 (in the Supporting Information), we present the predicted E_{HOMO}, E_{LUMO}, and E_g of the "CH"/N substituted derivatives. For a good interpretation of these results, a schematic representation for the energy levels of the HOMO and LUMO of the PF_n, OMC-CH_3, OMC-N_x, and OMC-NN_x ($x = 1$–4) is displayed in Fig. 6.

Table S5 and Fig. 6 clearly indicate that "CH"/N substitution in position(s) 7 (7 and 7′) decreases the E_{HOMO} (−5.21 and −5.37 eV), and increases the E_{LUMO} (−1.90 and −1.84 eV). Consequently, an increase is found for the E_g of OMC-N_1 and OMC-NN_1 (3.31 and 3.53 eV) as compared with that of OMC. "CH"/N substitution in position(s) 8 (8 and 8′) decreases the E_{HOMO} (−5.19 and −5.29 eV), while the prediction for E_{LUMO} being almost the same (−1.96 and −1.97 eV). Thus, the net effect is an increase of the E_g of OMC-N_2 and OMC-NN_2 as compared with that of OMC, the corresponding values being 3.23 and 3.32 eV. The very similar observation is also found for OMC-N_3 and OMC-NN_3. "CH"/N substitution in position(s) 10 (10 and 10′) decreases the E_{HOMO} (−5.20 and −5.31 eV), the E_{LUMO} being almost the same (−1.98 and −2.00 eV). As a consequence, the net effect is an increase in the E_g of OMC-N_3 and OMC-NN_3 in comparison with that of OMC, the corresponding values being 3.22 and 3.31 eV. Finally, "CH"/N substitution in position(s) 11 (11 and 11′) decreases both the E_{HOMO} (−5.18 and −5.25 eV) and E_{LUMO} (−2.06 and −2.13 eV) in comparison with that of OMC, giving the same E_g for OMC-N_4 and OMC-NN_4 (3.12 and 3.12 eV). These results indicate that the "CH"/N substitution should have certain effect on the energies of the FMOs depending on the position of the nitrogen substitution. In addition, the above results show, as compared with those of OMC, the magnitude of the variation for E_{HOMO}, E_{LUMO}, and E_g is in the increasing order of mono-substituted derivatives < di-substituted ones (except for E_g of OMC-N_4 and OMC-NN_4), indicating that di-substituted derivatives have more substituent effect than their corresponding mono-substituted counterparts owing to the presence of one more nitrogen atom. It should be noted that (shown in Fig. 6) the nitrogen substitution modified the HOMO and LUMO energy levels of the pristine molecule OMC. Nearly all the HOMO of the "CH"/N substituted derivatives are lowered in energy than that of the PF_n, indicating that charge trapping from PF_n to the "CH"/N substituted derivatives is not energetically favorable in the EL process.

It is instructive to analyze the HOMO and LUMO describing the lowest singlet excitation. We give the electronic density contours of the HOMO and LUMO for OMC-N_x and OMC-NN_x ($x = 1$–4) in Fig. 7. As visualized in Fig. 7, the LUMO show the same pattern, they are mainly localized on the central BTD ring (acceptor). A significant difference is however observed for the HOMO. The HOMO of OMC-N_x ($x = 1$–4) is found to be mostly localized on the triphenylamine

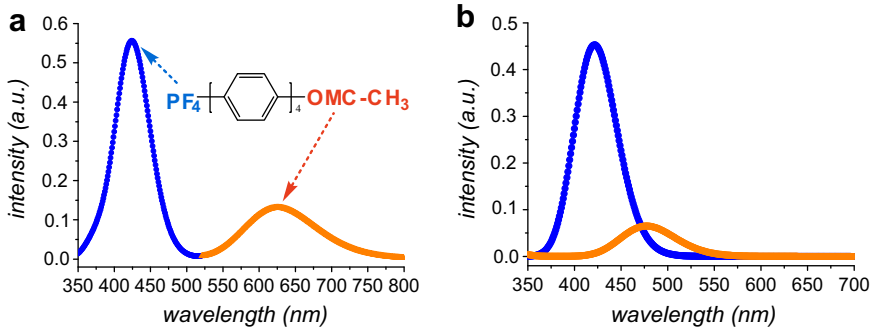

Fig. 5. (a) The emission spectrum of the copolymer. (b) Overlap of the simulated absorption spectrum of OMC-CH_3 and the simulated emission spectrum of PF_4. Blue: polymer host (PF_4); Orange: dopant (OMC-CH_3). [For interpretation of the references to colour in this figure legend, the reader is referred to the web version of this article.]

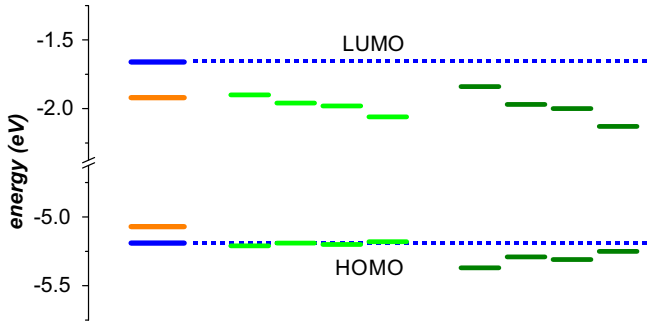

Fig. 6. Scheme of frontier molecular orbital levels. Blue: PF_n; Orange: OMC-CH_3; Green: OMC-N_x ($x = 1$–4, from left to right); Olive: OMC-NN_x ($x = 1$–4, from left to right). [For interpretation of the references to colour in this figure legend, the reader is referred to the web version of this article.]

unit without "CH"/N substitution instead of both units (observed for OMC-NN_x ($x = 1$–4) which seem to retain the HOMO characters in the pristine molecule OMC, as shown in Fig. S1 in the Supporting Information). The difference in the HOMO distribution of "CH"/N substituted derivatives can be understood from their S_0 geometries, since this geometric modification induces in turn changes in the electronic structure. From a careful analysis of the optimized results listed in Tables S7 and S8 (in the Supporting Information), one can find that, for OMC-N_x, all of the significant changes are located on the triphenylamine unit with "CH"/N substitution, the one without "CH"/N substitution remaining practically unaffected. As a consequence of the symmetry breaking, the HOMO of OMC-N_x are mainly localized on the triphenylamine unit without "CH"/N substitution instead of the one with "CH"/N substitution. This maybe implicate that the mono-substitution does not induce any significant contribution to the absorption transition and exists solely for the absolute energies of the FMOs. In OMC-NN_x, remarkable changes are observed in both triphenylamine units due to the symmetric substitution. As a consequence of the symmetry retaining, the HOMO of OMC-NN_x are mainly localized on both triphenylamine units. Fig. 7 also presents that, for HOMO, electron density localized on the triphenylamine unit with "CH"/N substitution slightly increases from OMC-N_1 to OMC-N_2, OMC-N_3 and then to OMC-N_4. A close examination of the optimized S_0 geometries of the OMC-N_x derivatives (see Tables S7 and S8, the Supporting Information) reveals a clue. Nitrogen substitutions in various positions have a distinct effect on the dihedral angles (C_3–C_4–C_6–C_7 and C_5–C_4–C_6–C_{11}) between the plane of the central BTD ring and the adjacent phenyl ring. "CH"/N substitution in position 7 (OMC-N_1) leads to more twisted structure (53.55° and 52.05°), mainly because of the steric repulsion between lone pair electrons of two nitrogens (N_2 and N_7), thus resulting in pronounced distortion from initial conformation (45.17° and 42.91°). As to OMC-N_2 and OMC-N_3, no significant changes are observed, whose predicted values (44.16°, 41.87° and 44.10°, 41.89°) only deviate by ca. 1.00° from the corresponding ones in OMC. "CH"/N substitution in position 11 (OMC-N_4) leads to much more planar structure (16.79° and 15.16°), which results from the relieving of the substantial steric repulsion between the two hydrogens located on C_5 and C_{11}. Therefore, for HOMO, electron density localized on the triphenylamine unit with "CH"/N substitution slightly increases from OMC-N_1 to OMC-N_2, OMC-N_3 and then to OMC-N_4 with the increasing of the degree of π conjugation between the central BTD ring and the adjacent phenyl ring.

3.2.2. Optical properties

Over the series, the first optical transition corresponds to a HOMO → LUMO (absorption process)/LUMO → HOMO (emission

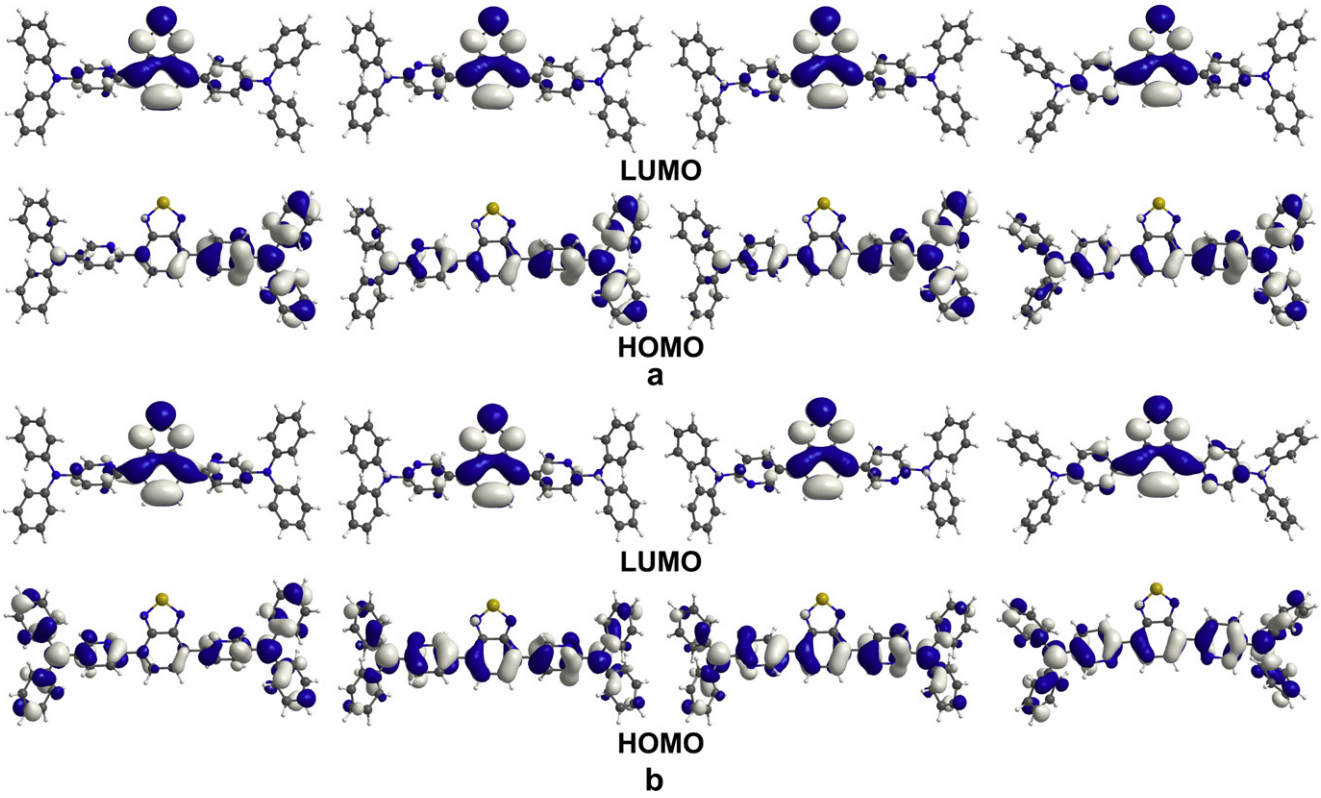

Fig. 7. (a) HOMO and LUMO of OMC-N_x ($x = 1$–4, from left to right). (b) HOMO and LUMO of OMC-NN_x ($x = 1$–4, from left to right).

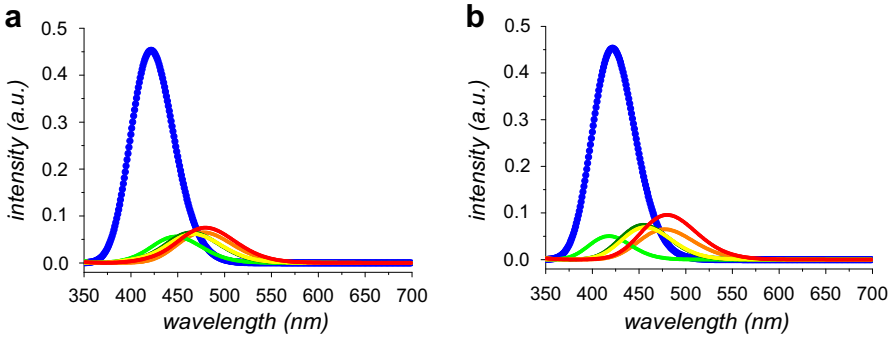

Fig. 8. (a) Overlap of the simulated absorption spectra of OMC-N_x and the simulated emission spectrum of PF_4. (b) Overlap of the simulated absorption spectra of OMC-NN_x and the simulated emission spectrum of PF_4. Blue: PF_4; Orange: OMC-CH_3; Green: OMC-N_1/OMC-NN_1; Olive: OMC-N_2/OMC-NN_2; Yellow: OMC-N_3/OMC-NN_3; Red: OMC-N_4/OMC-NN_4. [For interpretation of the references to colour in this figure legend, the reader is referred to the web version of this article.]

process) excitation. The distribution patterns of the HOMO and LUMO provide a remarkable signature for the charge transfer character of the transition.

Within "CH"/N substituted derivatives (OMC-N_x and OMC-NN_x, $x = 1$–4), in comparison with that of OMC (471.2 nm), remarkable blue shifts of ca. 22.2 and 53.4 nm are predicted for OMC-N_1 and OMC-NN_1 λ_{abs} (449.0 and 417.8 nm) respectively, while for OMC-N_2, OMC-N_3, OMC-NN_2, and OMC-NN_3, relatively slight blue shifts of ca. 5.9, 3.9, 16.6, 14.4 nm are predicted for their λ_{abs} (465.3, 467.3, 454.6, 456.8 nm). On the other side, red shifts of ca. 9.4 and 9.1 nm are predicted on λ_{abs} for OMC-N_4 and OMC-NN_4 (480.6 and 480.3 nm), respectively. It can be also found from Table 2 that, the λ_{em} predicted for "CH"/N substituted derivatives are blue shifted with respect to that of OMC (617.1 nm). Significant λ_{em} blue shifts of ca. 46.8 and 77.7 nm are observed for OMC-N_1 and OMC-NN_1 (570.3 and 539.4 nm), whereas relatively slight λ_{em} blue shifts of ca. 9.6, 2.7, 7.4, 21.6, 8.0, 14.5 nm are observed for OMC-N_2, OMC-N_3, OMC-N_4, OMC-NN_2, OMC-NN_3, and OMC-NN_4 (607.5, 614.4, 609.7, 595.5, 609.1, 602.6 nm). From these results, it is obvious that di-substituted derivatives show shorter maximal absorption/emission wavelength than their corresponding mono-substituted counterparts. In Table S9 (in the Supporting Information), we show the correlation between the $\lambda_{abs}/\lambda_{em}$ and the E_g for two series of derivatives. Inspection of Table S9 (in the Supporting Information) reveals that the smaller E_g is, the more obvious the red shifts in $\lambda_{abs}/\lambda_{em}$ are. The change for $\lambda_{abs}/\lambda_{em}$ can be simply traced back to the variation of E_g because the first optical transition corresponds to a HOMO → LUMO/LUMO → HOMO excitation. In Fig. 8, the overlap of the emission spectrum of PF_4 with the absorption spectra of "CH"/N substituted derivatives is presented. As Fig. 8 shows, blue/red shifts of the absorption spectra upon nitrogen substitution lead to increases/decreases of the overlap. Although pure "CH"/N substituted derivatives are not appropriated for the orange dopants in WPLEDs with PF_n as a blue-light-emitting host because their HOMO and LUMO energy levels do not match well with those of the PF_n, this work may provide a new means for experimentalists to design new yellow and orange light-emitting materials on the basis of their emission spectra (539.4–614.4 nm) calculated in the gas phase. In the following sections, we should find an efficient way to modify the electronic and optical properties of the "CH"/N substituted derivatives, with the aim to develop orange dopants for WPLEDs applications in which PF_n is as a blue-light-emitting host.

3.3. H/R substituted derivatives for OMC-N_x/OMC-NN_x

In general, changes in the molecular structure lead to a possible modulation of the electronic energy levels and hence of the optical properties. From the theoretical standpoint, the electron-donor strength can be related to the E_{HOMO} of a molecule. On the basis of OMC-N_x and OMC-NN_x ($x = 1$–4), therefore, the commonly known electron-donating groups [–CH_3, –OCH_3, –NH_2, and –$N(CH_3)_2$] are selectively introduced on *N*,*N*-disubstituted amino groups (shown in Fig. 1b). It is interesting to know how this strategy may tune the HOMO levels in the corresponding "CH"/N substituted derivatives.

3.3.1. Electronic properties

Table S5 (in the Supporting Information) summarizes the E_{HOMO}, E_{LUMO} and E_g for the H/R substituted derivatives based on the OMC-N_x and OMC-NN_x ($x = 1$–4). For a better interpretation of these results, the trends of the results are schematically plotted in Fig. 9.

First of all, a same trend is observed for the variation of the E_{HOMO}, E_{LUMO}, and E_g in these two series of derivatives. Since –CH_3, –OCH_3, –NH_2, and –$N(CH_3)_2$ are electron-donating groups, they push the electron to the parent ring and increase the p_π electron density. In general, the effect of the addition of an electron-donating group to a conjugated system is to raise the E_{HOMO} and E_{LUMO}. Indeed, all of the substitutions enable the HOMO and LUMO

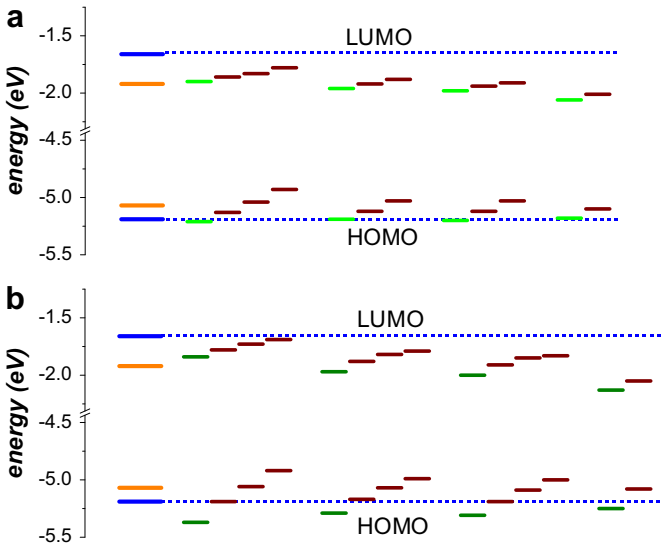

Fig. 9. Scheme of frontier molecular orbital levels. (a) OMC-N_x/OMC-N_x-R; (b) OMC-NN_x/OMC-NN_x-R. Blue: PF_n; Orange: OMC-CH_3; Green: OMC-N_x ($x = 1$–4, from left to right); Olive: OMC-NN_x ($x = 1$–4, from left to right); Wine: OMC-N_x-R/OMC-NN_x-R. [For interpretation of the references to colour in this figure legend, the reader is referred to the web version of this article.]

energy levels increase in contrast to the corresponding "CH"/N substituted derivatives. The E_{HOMO} increased more than E_{LUMO}, thus the E_g decreases with respect to the corresponding derivatives without substituents. The substituent effect with the electron-donating groups has the following order: $-CH_3 < -OCH_3 < -NH_2 < -N(CH_3)_2$. Taking OMC-$NN_1$-R (R = $-OCH_3$, $-NH_2$, $-N(CH_3)_2$) as examples, going from OMC-NN_1-OCH_3 to OMC-NN_1-NH_2, and then to OMC-NN_1-$N(CH_3)_2$, the E_{HOMO} is predicted in the increasing order of $-5.19 < -5.06 < -4.92$ eV and the E_{LUMO} in the order of $-1.78 < -1.73 < -1.69$ eV. As a result, our prediction shows a decreasing E_g in the order of $3.41 > 3.33 > 3.23$ eV. From Fig. 9 it is clearly shown that E_{HOMO} and E_{LUMO} of "CH"/N substituted derivatives can be efficiently tuned with different electron-donating groups on *N*,*N*-disubstituted amino units.

In Fig. 10, we give the electronic density contours of the HOMO and LUMO for OMC-N_1-R (R = $-CH_3$, $-OCH_3$, and $-NH_2$) and OMC-NN_1-R (R = $-OCH_3$, $-NH_2$, and $-N(CH_3)_2$) as representatives of the derivatives under investigation, the others being plotted in Fig. S2 (in the Supporting Information). As shown in Fig. 10 and Fig. S2, we find that a similar description of the electronic structure for H/R substituted derivatives and the corresponding ones without substituents. The HOMO of OMC-N_x-R ($x = 1$–4) is found to be mostly localized on the triphenylamine unit without "CH"/N substitution, while for OMC-NN_x-R ($x = 1$–4), the HOMO are mainly localized on both triphenylamine units. The LUMO show the same pattern; they are mainly localized on the central BTD ring. It is important to note that all of the substituents interact mainly with the HOMO, whereas their interaction with the LUMO is very little.

3.3.2. Optical properties

Analogous to the "CH"/N derivatives, OMC-N_x-R and OMC-NN_x-R derivatives show strong charge transfer for the HOMO → LUMO (absorption process) and LUMO → HOMO (emission process) transition.

Table 3 presents a general trend that the λ_{abs} exhibit red shifts on introducing the electron-donating groups with respect to the corresponding "CH"/N substituted derivatives. The red shift upon substitution increases in the following order: $-CH_3 < -OCH_3 < -NH_2 < -N(CH_3)_2$. Taking OMC-$NN_1$-R (R = $-OCH_3$, $-NH_2$, $-N(CH_3)_2$) as examples, as the strength of the donors increases from $-OCH_3$ to $-NH_2$, and then to $-N(CH_3)_2$, the λ_{abs} prediction shows the

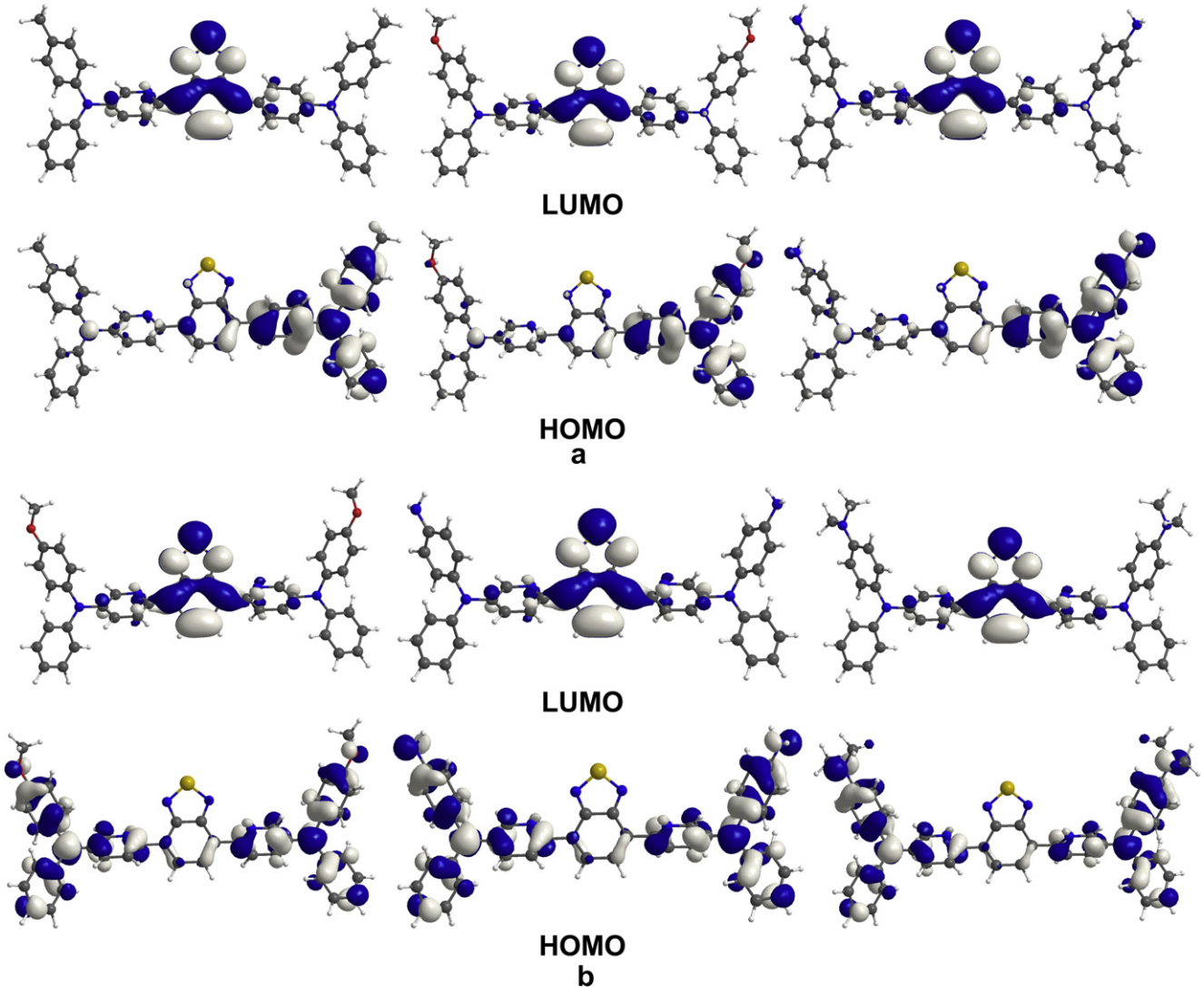

Fig. 10. (a) HOMO and LUMO of OMC-N_1-R (R = $-CH_3$, $-OCH_3$, $-NH_2$, from left to right). (b) HOMO and LUMO of OMC-NN_1-R (R = $-OCH_3$, $-NH_2$, $-N(CH_3)_2$, from left to right).

Table 3
Optical properties of OMC-N_x/OMC-N_x-R and OMC-NN_x/OMC-NN_x-R ($x = 1$–4) computed at the TD-PBE0/6-31G(d) level.

	Absorption Properties						Emission Properties					
	Gas			CH_2Cl_2			Gas			CH_2Cl_2		
	E_v	λ_{abs}	f	E_v	λ_{abs}	f	E_v	λ_{em}	f	E_v	λ_{em}	f
OMC-N_x/OMC-N_x-R												
OMC-N_1	2.76	449.0	0.38	2.65	468.4	0.39	2.17	570.3	0.95	2.01	616.0	1.01
OMC-N_1-CH_3	2.73	454.6	0.38	2.61	475.1	0.40	2.15	575.9	0.96	1.99	622.4	1.02
OMC-N_1-OCH_3	2.67	463.8	0.37	2.56	484.3	0.39	2.12	584.0	0.95	1.96	631.9	1.00
OMC-N_1-NH_2	2.62	473.6	0.36	2.46	504.5	0.37	2.09	593.0	0.93	1.90	652.5	0.98
OMC-N_2	2.66	465.3	0.44	2.60	476.4	0.46	2.04	607.5	0.78	1.95	636.8	0.87
OMC-N_2-CH_3	2.64	470.5	0.44	2.57	482.3	0.45	2.02	612.6	0.79	1.93	642.1	0.88
OMC-N_2-OCH_3	2.59	478.0	0.41	2.53	489.9	0.43	2.00	618.7	0.77	1.91	648.9	0.86
OMC-N_3	2.65	467.3	0.42	2.60	476.9	0.44	2.02	614.4	0.75	1.93	641.2	0.86
OMC-N_3-CH_3	2.62	472.4	0.42	2.57	482.6	0.44	2.00	619.6	0.76	1.92	646.6	0.87
OMC-N_3-OCH_3	2.58	481.0	0.40	2.53	490.9	0.41	1.98	627.0	0.75	1.90	654.2	0.85
OMC-N_4	2.58	480.6	0.51	2.49	497.4	0.57	2.03	609.7	0.83	1.91	647.6	0.95
OMC-N_4-CH_3	2.55	486.5	0.52	2.46	504.1	0.58	2.01	615.7	0.84	1.90	654.2	0.95
OMC-NN_x/OMC-NN_x-R												
OMC-NN_1	2.97	417.8	0.35	2.78	445.6	0.33	2.30	539.4	1.11	2.09	593.3	1.13
OMC-NN_1-OCH_3	2.86	433.2	0.33	2.68	462.9	0.32	2.24	553.1	1.10	2.03	610.5	1.11
OMC-NN_1-NH_2	2.80	443.5	0.32	2.56	485.1	0.29	2.21	561.9	1.09	1.96	632.9	1.08
OMC-NN_1-$N(CH_3)_2$	2.72	455.0	0.30	2.50	495.7	0.27	2.17	572.3	1.08	1.93	643.4	1.06
OMC-NN_2	2.73	454.6	0.51	2.69	460.8	0.56	2.08	595.5	0.77	2.01	617.6	0.86
OMC-NN_2-OCH_3	2.70	459.8	0.51	2.66	466.1	0.54	2.06	602.6	0.77	1.98	624.8	0.86
OMC-NN_2-NH_2	2.67	464.7	0.49	2.60	477.6	0.51	2.04	608.5	0.76	1.94	638.4	0.84
OMC-NN_2-$N(CH_3)_2$	2.63	471.5	0.49	2.57	483.1	0.50	2.01	615.5	0.78	1.93	643.4	0.85
OMC-NN_3	2.71	456.8	0.48	2.69	460.2	0.54	2.04	609.1	0.72	1.98	626.0	0.84
OMC-NN_3-OCH_3	2.68	462.0	0.48	2.66	465.7	0.52	2.01	616.8	0.73	1.96	633.4	0.84
OMC-NN_3-NH_2	2.65	467.6	0.46	2.59	478.2	0.49	1.99	622.7	0.71	1.91	647.5	0.82
OMC-NN_3-$N(CH_3)_2$	2.61	475.9	0.45	2.56	484.8	0.47	1.96	631.9	0.74	1.90	653.8	0.84
OMC-NN_4	2.58	480.3	0.66	2.46	503.6	0.74	2.06	602.6	0.84	1.93	643.7	0.98
OMC-NN_4-OCH_3	2.51	494.4	0.65	2.39	518.8	0.72	2.01	617.0	0.84	1.88	660.7	0.97

E_v = the vertical excitation energies (in eV). $\lambda_{abs}/\lambda_{em}$ = the maximum absorption/emission wavelength (in nm). f = the oscillator strength.

increasing order of 433.2 < 443.5 < 455.0 nm. The same observation is also found for λ_{em}. The results displayed in Table S9 (in the Supporting Information) reveal that, the trend in $\lambda_{abs}/\lambda_{em}$ is directly correlated to the E_g because the $S_0 \rightarrow S_1/S_1 \rightarrow S_0$ transition is mainly described by an electronic excitation from the HOMO to the LUMO levels/from the LUMO to the HOMO levels. On the basis of the emission spectra calculated in the gas phase (553.1–631.9 nm), we predict that H/R substituted derivatives can be used as yellow and orange light-emitting materials. Fig. 11 shows the overlap between the emission spectrum of PF_4 and the absorption spectra of H/R and the corresponding "CH"/N substituted derivatives. It is found that red shifts of the absorption spectra upon H/R substitution lead to decreases of the overlap. Moreover, the results indicate that the HOMO and LUMO energy levels of these H/R substituent derivatives lie within the range of the band gap of the PF_n (shown in Fig. 9). These results presented in this section show that the introduction of electron-donating groups to the "CH"/N substituted derivatives is a highly effective way to develop orange dopants for WPLEDs applications in which PF_n is as a blue-light-emitting host.

3.4. Solvent effects on the electronic and optical properties of the OMC-based derivatives

The solvent effects are receiving considerable attention as most of the chemical processes occur in solution phase. The solvent effects are included in the calculations to ensure the calculations are compatible with the typical experimental conditions under which the optical and electrochemical properties are measured. The influence of the chemical environment is discussed further below.

The combined calculations of DFT (PBE0) and PCM on the investigated BTD-based derivatives are carried out on the HF/6-31G(d) gas-phase optimized geometries to explore the electronic properties in the dichloromethane solution. The calculated E_{HOMO}, E_{LUMO}, and E_g are listed in Tables S5, the Supporting Information. Including dichloromethane effects induces the lowering in the HOMO and LUMO energy levels and the decreasing in the E_g (except for OMC-NN_2, OMC-NN_3 and OMC-NN_3-OCH_3). In Fig. 12, we show the HOMO and LUMO of OMC-CH_3, OMC-N_1, and OMC-NN_1 as representatives of the series of the derivatives under this study, the others being plotted in Fig. S3 (in the Supporting Information). It is worth noting that all the HOMO and LUMO of OMC-CH_3, OMC-N_1, and OMC-NN_1 in dichloromethane have very similar appearance to the corresponding orbitals in the gas phase (shown in Figs. 4, 7, and 12). These features strongly indicate that inclusion of the solvent effect does not change the nature of the FMOs, but exists solely for the obvious shift in absolute energy.

In addition, the TD–DFT (PBE0) spectral calculations have been performed on the HF/6-31G(d) and CIS/6-31G(d) gas-phase optimized geometries using the PCM description of dichloromethane. The results for absorption and emission transitions are given in Tables 2 and 3. Compared with that of in the gas phase, the introduction of the solvent effects (PCM model) in our TD–DFT calculation leads to red shifts for all λ_{abs} and λ_{em} values, that can be estimated to ~3–42 nm and ~17–71 nm respectively, which indicates that the impact of the medium on the optical properties is to be larger for the emission spectra than for the absorption ones. The λ_{em} of these designed BTD-based derivatives are located at yellow to red scope (593.3–660.7 nm), implying that they can be used as yellow to red light-emitting materials involving the environmental influences. The maximum absorption/emission wavelength still corresponds to the charge transfer transition involved in the gas phase, i.e., to the HOMO → LUMO/LUMO → HOMO electronic excitation. It may be reasonable to conclude that, when

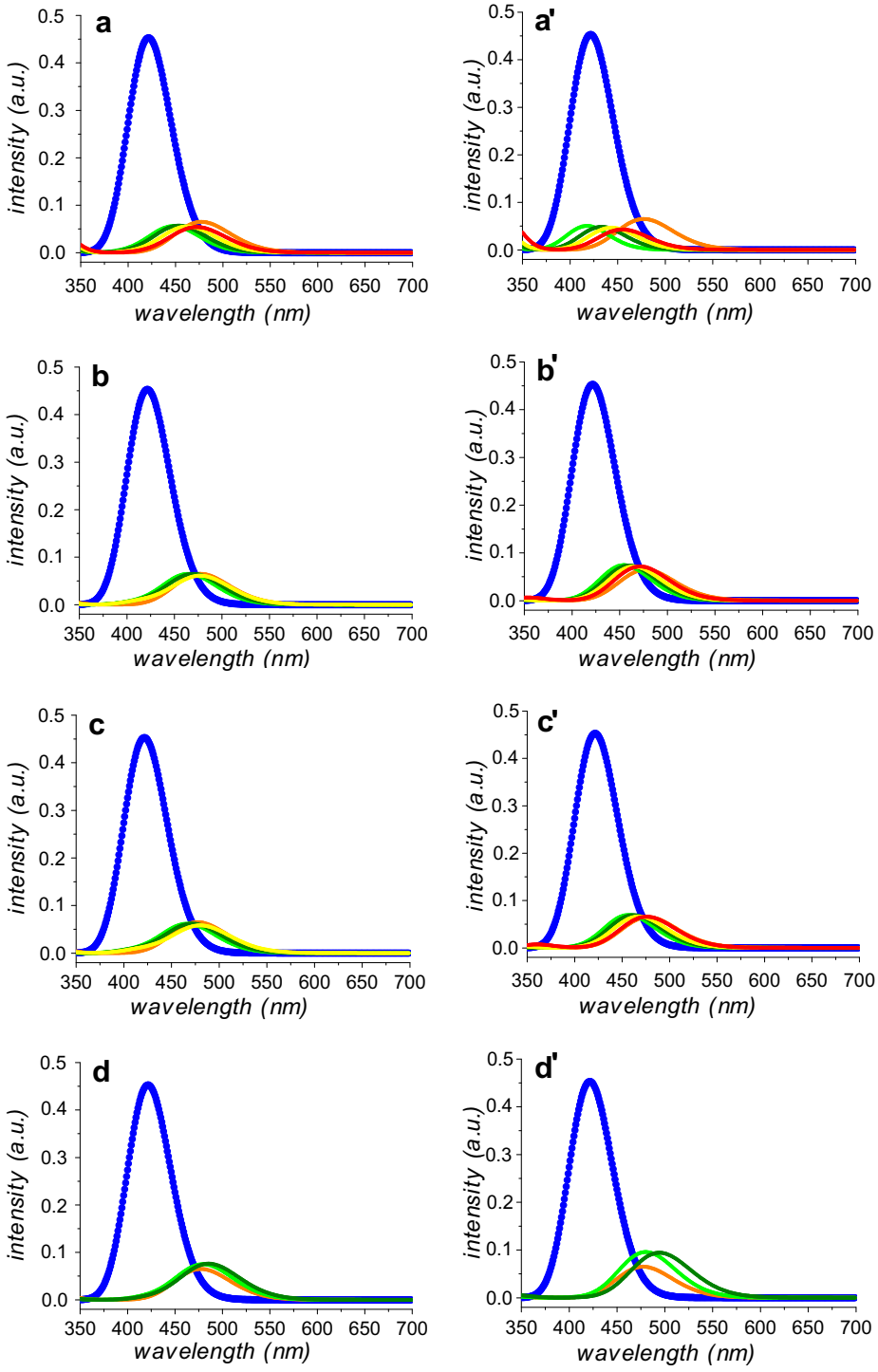

Fig. 11. (a–d) Overlap of the simulated absorption spectra of OMC-N_x-R ($x = 1$–4) and the simulated emission spectrum of PF_4. (a′–d′) Overlap of the simulated absorption spectra of OMC-NN_x-R ($x = 1$–4) and the simulated emission spectrum of PF_4. Blue: PF_4; Orange: OMC-CH_3; Green: OMC-N_x/OMC-NN_x; Olive: OMC-N_x-CH_3/OMC-NN_x-OCH_3; Yellow: OMC-N_x-OCH_3/OMC-NN_x-NH_2; Red: OMC-N_x-NH_2/OMC-NN_x-$N(CH_3)_2$. [For interpretation of the references to colour in this figure legend, the reader is referred to the web version of this article.]

accounting for the solvent effects, only the λ_{abs} and λ_{em} numerical values significantly increase, whereas the transition character does not reveal any changes.

3.5. Reorganization energy

Our calculations of the reorganization energy associated with different geometries of two states are based on the hopping model schematically illustrated in Fig. 13. For each molecule, the geometry is optimized for both the neutral and the cationic/anionic states at the PBE0/6-31G(d) level. The energies corresponding to the neutral and cationic/anionic electronic configurations are then computed for each of the two optimized geometrical structures at the B3LYP/6-31G(d,p) level in order to compare with the values available [54–56]. The results are summarized in Table 4. The reorganization energies computed for hole (λ_h in the range of 0.168–0.287 eV) are

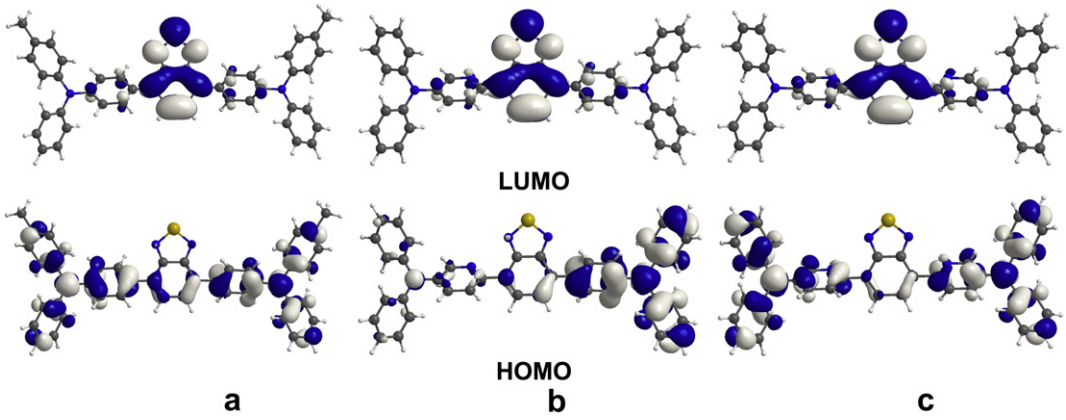

Fig. 12. HOMO and LUMO of (a) OMC-CH_3; (b) OMC-N_1; (c) OMC-NN_1 considering solvent effects.

all smaller than that of N,N′-diphenyl-N,N′-bis(3-methlphenyl)-(1,1′-biphenyl)-4,4′-diamine (TPD) which is a typical hole transport material ($\lambda_h = 0.290$ eV) [55], while for electron λ_e (between 0.446 and 0.613 eV), they are much larger than that of tris(8-hydroxyquinolinato)aluminum(III) (Alq_3) which is a typical electron transport material ($\lambda_e = 0.276$ eV) [56]. The smaller λ value is, the bigger the charge transport rate is. λ_h are all smaller than their respective λ_e, suggesting that the carrier mobility of the hole is larger than that of the electron. It indicates that BTD-based derivatives explored in this work can be used as better hole transport materials in the organic light-emitting diodes (OLEDs) from the stand point of the smaller reorganization energy. The data in Table 4 show that, λ_h of OMC-N_x and OMC-NN_x ($x = 1$–4) decrease (in the range of 0.168–0.222 eV) in comparison with that of OMC (0.230 eV), indicating the hole transportation is improved with the "CH"/N substitution. Moreover, λ_h of the di-substituted derivatives (0.220, 0.168, 0.177, 0.192 eV) are smaller than their corresponding mono-substituted counterparts (0.222, 0.199, 0.205, 0.215 eV), implying that there is a relationship between λ_h and the number of nitrogen atoms. Table 4 also presents, in comparison with that of the corresponding "CH"/N substituted derivatives, introducing –CH_3 and –OCH_3 groups on *N*,*N*-disubstituted amino groups result in a decrease of λ_h, except for OMC-NN_2-OCH_3 and OMC-NN_3-OCH_3. It suggests that –CH_3 and –OCH_3 substitution lead to further improvement for hole transportation. However, λ_h significantly increase when introducing –NH_2 and –$N(CH_3)_2$ groups on *N*,*N*-disubstituted amino groups, indicating that –NH_2 or –$N(CH_3)_2$ substitution has no positive effect on hole transportation.

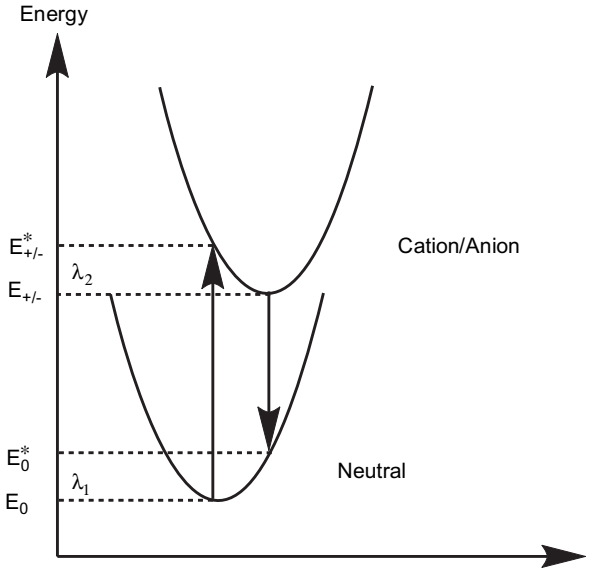

Fig. 13. Sketch of the potential energies of neutral and cation/anion species, illustrating the neutral (λ_1) and cation/anion (λ_2) relaxation energies.

Table 4
Intramolecular reorganization energies (in eV) of OMC, OMC-CH_3, OMC-N_x/OMC-N_x-R, and OMC-NN_x/OMC-NN_x-R ($x = 1$–4) computed at the B3LYP/6-31G(d,p)//PBE0/6-31G(d) level.

	Reorganization for hole			Reorganization for electron		
	λ_{h1}	λ_{h2}	$\lambda_h = \lambda_{h1} + \lambda_{h2}$	λ_{e1}	λ_{e2}	$\lambda_e = \lambda_{e1} + \lambda_{e2}$
Pristine						
OMC	0.143	0.087	0.230	0.176	0.322	0.498
OMC-CH_3	0.146	0.059	0.205	0.191	0.321	0.512
OMC-N_x/OMC-N_x-R						
OMC-N_1	0.145	0.077	0.222	0.203	0.343	0.546
OMC-N_1-CH_3	0.134	0.065	0.199	0.211	0.342	0.553
OMC-N_1-OCH_3	0.131	0.066	0.197	0.231	0.342	0.573
OMC-N_1-NH_2	0.163	0.105	0.268	0.230	0.348	0.578
OMC-N_2	0.127	0.072	0.199	0.201	0.321	0.522
OMC-N_2-CH_3	0.115	0.063	0.178	0.208	0.312	0.520
OMC-N_2-OCH_3	0.114	0.069	0.183	0.182	0.304	0.486
OMC-N_3	0.132	0.073	0.205	0.205	0.327	0.532
OMC-N_3-CH_3	0.131	0.059	0.190	0.220	0.333	0.553
OMC-N_3-OCH_3	0.125	0.066	0.191	0.206	0.328	0.534
OMC-N_4	0.145	0.070	0.215	0.183	0.289	0.472
OMC-N_4-Me	0.130	0.061	0.191	0.202	0.325	0.527
OMC-NN_x/OMC-NN_x-R						
OMC-NN_1	0.151	0.069	0.220	0.239	0.347	0.586
OMC-NN_1-OCH_3	0.141	0.059	0.200	0.220	0.332	0.552
OMC-NN_1-NH_2	0.178	0.109	0.287	0.268	0.345	0.613
OMC-NN_1-$N(CH_3)_2$	0.136	0.109	0.245	0.238	0.329	0.567
OMC-NN_2	0.109	0.059	0.168	0.191	0.305	0.496
OMC-NN_2-OCH_3	0.109	0.070	0.179	0.190	0.311	0.501
OMC-NN_2-NH_2	0.146	0.108	0.254	0.193	0.319	0.512
OMC-NN_2-$N(CH_3)_2$	0.121	0.127	0.248	0.194	0.326	0.520
OMC-NN_3	0.123	0.054	0.177	0.233	0.331	0.564
OMC-NN_3-OCH_3	0.123	0.065	0.188	0.208	0.301	0.509
OMC-NN_3-NH_2	0.158	0.103	0.261	0.207	0.316	0.523
OMC-NN_3-$N(CH_3)_2$	0.130	0.105	0.235	0.176	0.270	0.446
OMC-NN_4	0.123	0.069	0.192	0.194	0.303	0.497
OMC-NN_4-OCH_3	0.117	0.059	0.176	0.209	0.307	0.516
Pentacene			0.098[a]			
TPD			0.290[b]			
Alq_3						0.276[c]

[a] Reference data from Ref. [54].
[b] Reference data from Ref. [55].
[c] Reference data from Ref. [56].

4. Conclusions

Using ab initio and DFT approaches, we investigate the white-light emission from a single-polymer system with simultaneous blue (PF_n as a blue host) and orange (a BTD-based derivative as an orange dopant) emission. Good consistency is found between the calculated results and available experimental data. The influence of the "CH"/N heterosubstitution of the spacer part on the electronic and optical properties of the BTD-based derivatives is considered. Compared with the pristine molecule OMC, "CH"/N substitution has an effect on the energies of the FMOs depending on the position of the nitrogen substitution. Di-substituted derivatives have more substituent effect than their corresponding mono-substituted counterparts. Moreover, the distribution patterns of HOMO of mono-substituted derivatives are found to be mostly localized on the triphenylamine unit without "CH"/N substitution instead of both units (observed for di-substituted derivatives which seem to retain the HOMO characters in the pristine molecule OMC). This suggests that the mono-substitution does not induce any significant contribution to the absorption transition and exists solely for the absolute energies of the FMOs. The change of $\lambda_{abs}/\lambda_{em}$ for these "CH"/N substitution derivatives can be simply traced back to the variation of E_g because the first optical transition corresponds to a HOMO → LUMO/LUMO → HOMO excitation. Although "CH"/N substituted derivatives are not appropriated for the orange dopants in WPLEDs with PF_n as a blue-light-emitting host, this work may provide a new means for experimentalists to design new yellow and orange light-emitting materials. In addition, we find that the electronic and optical properties of "CH"/N substitution derivatives can be tuned by symmetrically adding suitable electron-donating groups [$-CH_3$, $-OCH_3$, $-NH_2$, and $-N(CH_3)_2$] on *N*,*N*-disubstituted amino groups, suggesting them to be good candidates as orange dopants in WPLEDs with PF_n as a blue-light-emitting host. The dichloromethane solvation effects on the electronic and optical properties of BTD-based derivatives leads to the lowering in the HOMO and LUMO energy levels, the decreasing in the energy gap (except for OMC-NN_2, OMC-NN_3 and OMC-NN_3-OCH_3), as well as red shifts for absorption and emission spectra. A series of low reorganization energy values (λ_h) are also obtained based on the BTD-based derivatives under study, indicating that these derivatives can be used as better hole transport materials in the OLEDs. We expect that the theoretical investigation of the electronic and optical properties for these light-emitting derivatives will help to design more efficient functional molecules.

Acknowledgments

Financial supports from the NSFC (Nos. 50873020, 20773022), NENU-STB07007, and NCET-06-0321 are gratefully acknowledged.

References

[1] Kido J, Kimura M, Nagai K. Science 1995;267:1332.
[2] (a) Strukelj M, Jordan RH, Dodabalapur A. J Am Chem Soc 1996;118:1213;
(b) Jordan RH, Dodabalapur A, Strukelj M, Miller TM. Appl Phys Lett 1996;68:1192.
[3] Shen Z, Burrows PE, Bulovic V, Forrest SR, Thompson ME. Science 1997;276:2009.
[4] Xie ZY, Huang JS, Li CN, Liu SY, Wang Y, Li YQ, et al. Appl Phys Lett 1999;74:641.
[5] Steuber F, Staudigel J, Stössel M, Simmerer J, Winnacker A, Spreitzer H, et al. Adv Mater 2000;12:130.
[6] (a) Lee YZ, Chen X, Chen MC, Chen SA, Hsu JH, Fann W. Appl Phys Lett 2001;79:308;
(b) Ko CW, Tao YT. Appl Phys Lett 2001;79:4234.
[7] (a) D'Andrade BW, Thompson ME, Forrest SR. Adv Mater 2002;14:147;
(b) D'Andrade BW, Brooks J, Adamovich V, Thompson ME, Forrest SR. Adv Mater 2002;14:1032.
[8] Totiko S, Lijima T, Tsuzuki T, Sato F. Appl Phys Lett 2003;83:2459.
[9] (a) Furuta PT, Deng L, Garon S, Thompson ME, Fréchet JMJ. J Am Chem Soc 2004;126:15388;
(b) D'Andrade BW, Holmes RJ, Forrest SR. Adv Mater 2004;16:624;
(c) Li JY, Liu D, Ma C, Lengyel O, Lee CS, Tung CH, et al. Adv Mater 2004;16:1538.
[10] Mazzeo M, Vitale V, Sala FD, Anni M, Barbarella G, Favaretto L, et al. Adv Mater 2005;17:34.
[11] (a) Sun YR, Giebink NC, Kanno H, Ma BW, Thompson ME, Forrest SR. Nature 2006;440:908;
(b) Liu Y, Nishiura M, Wang Y, Hou ZM. J Am Chem Soc 2006;128:5592;
(c) Yu XM, Kwok HS, Wong WY, Zhou GJ. Chem Mater 2006;18:5097;
(d) Kanno H, Holmes RJ, Sun Y, Kena-Cohen S, Forrest SR. Adv Mater 2006;18:339.
[12] (a) You YM, Kim KS, Ahn TK, Kim DH, Park SY. J Phys Chem C 2007;111:4052;
(b) Williams EL, Haavisto K, Li J, Jabbour GE. Adv Mater 2007;19:197;
(c) Niu YH, Liu MS, Ka JW, Bardeker J, Zin MT, Schofield R, et al. Adv Mater 2007;19:300;
(d) Yan BP, Cheung CCC, Kui SCF, Xiang HF, Roy VAL, Xu SJ, et al. Adv Mater 2007;19:3599.
[13] (a) Kulkarni AP, Jenekhe SA. J Phys Chem C 2008;112:5174;
(b) Zhao ZJ, Xu B, Yang ZF, Wang HY, Wang XM, Lu P, et al. J Phys Chem C 2008;112:8511;
(c) Park YS, Kang JW, Kang DM, Park JW, Kim YH, Kown SK, et al. Adv Mater 2008;20:1957;
(d) Su SJ, Gonmori E, Sasabe H, Kido J. Adv Mater 2008;20:4189;
(e) Ho CL, Wong WY, Wang Q, Ma DG, Wang LX, Lin ZY. Adv Funct Mater 2008;18:928;
(f) Tao SL, Zhou YC, Lee CS, Lee ST, Huang D, Zhang XH. J Mater Chem 2008;18:3981.
[14] (a) Fadhel O, Gras M, Lemaitre N, Deborde V, Hissler M, Geffroy B, et al. Adv Mater 2009;21:1261;
(b) Vijayakumar C, Praveen VK, Ajayaghosh A. Adv Mater 2009;21:2059;
(c) Wang Q, Ding JQ, Ma DG, Cheng YX, Wang LX, Wang FS. Adv Mater 2009;21:2397;
(d) Wang Q, Ding JQ, Ma DG, Cheng YX, Wang LX, Jing XB, et al. Adv Funct Mater 2009;19:84;
(e) Lin ZH, Wen YS, Chow TJ. J Mater Chem 2009;19:5141;
(f) Wang Q, Ding JQ, Ma DG, Cheng YX, Wang LX. Appl Phys Lett 2009;94:103503.
[15] (a) Gong X, Moses D, Heeger AJ, Xiao S. J Phys Chem B 2004;108:8601;
(b) Gong X, Ma W, Ostrowski JC, Bazan GC, Moses D, Heeger AJ. Adv Mater 2004;16:615;
(c) Gong X, Wang S, Moses D, Bazan GC, Heeger AJ. Adv Mater 2005;17:2053;
(d) Huang JS, Li G, Wu E, Xu QF, Yang Y. Adv Mater 2006;18:114;
(e) Wu HB, Zou JH, Liu F, Wang L, Mikhailovsky A, Bazan GC, et al. Adv Mater 2008;20:696;
(f) Shih PI, Tseng YH, Wu FI, Dixit AK, Shu CF. Adv Funct Mater 2006;16:1582;
(g) Granström M, Inganäs O. Appl Phys Lett 1996;68:147;
(h) Tasch S, List EJW, Ekström O, Graupner W, Leising G, Schlichting P, et al. Appl Phys Lett 1997;71:2883;
(i) Ho GK, Meng HF, Lin SC, Horng SF, Hsu CS, Chen LC, et al. Appl Phys Lett 2004;85:4576;
(j) Xu YH, Peng JB, Mo YQ, Hou Q, Cao Y. Appl Phys Lett 2005;86:163502;
(k) Chen FC, Chien SC, Chen YS. Appl Phys Lett 2009;94:043306.
[16] (a) Wu HB, Zhou GJ, Zou JH, Ho CL, Wong WY, Yang W, et-al. Adv Mater, in press;
(b) Kim TH, Lee HK, Park OO, Chin BD, Lee SH, Kim JK. Adv Funct Mater 2006;16:611;
(c) Kido J, Hongawa K, Okuyama K, Nagai K. Appl Phys Lett 1994;64:815;
(d) Kido J, Shionoya H, Nagai K. Appl Phys Lett 1995;67:2281;
(e) Kamata N, Ishii R, Tonsyo S, Terunuma D. Appl Phys Lett 2002;81:4350;
(f) Kim JH, Herguth P, Kang MS, Jen AKY, Tseng YH, Shu CF. Appl Phys Lett 2004;85:1116;
(g) Xu Q, Duong HM, Wudl F, Yang Y. Appl Phys Lett 2004;85:3357;
(h) Shih PI, Shu CF, Tung YL, Chi Y. Appl Phys Lett 2006;88:251110;
(i) Huang JS, Hou WJ, Li JH, Li G, Yang Y. Appl Phys Lett 2006;89:133509;
(j) Fan SQ, Sun ML, Wang J, Yang W, Cao Y. Appl Phys Lett 2007;91:213502.
[17] (a) Gebler DD, Wang YZ, Blatchford JW, Jessen SW, Fu DK, Swager TM, et al. Appl Phys Lett 1997;70:1644;
(b) Chao CL, Chen SA. Appl Phys Lett 1998;73:426;
(c) Mazzeo M, Pisignano D, Della Sala F, Thompson J, Blyth RIR, Gigli G, et al. Appl Phys Lett 2003;82:334;
(d) Sun QJ, Fan BH, Tan ZA, Yang CH, Li YF, Yang Y. Appl Phys Lett 2006;88:163510.
[18] (a) Liu J, Zhou QG, Cheng YX, Geng YH, Wang LX, Ma DG, et al. Adv Mater 2005;17:2974;
(b) Liu J, Xie ZY, Cheng YX, Geng YH, Wang LX, Jing XB, et al. Adv Mater 2007;19:531;
(c) Liu J, Chen L, Shao SY, Xie ZY, Cheng YX, Geng YH, et al. Adv Mater 2007;19:4224.
[19] (a) Tu GL, Zhou QG, Cheng YX, Wang LX, Ma DG, Jing XB, et al. Appl Phys Lett 2004;85:2172;
(b) Tu GL, Mei CY, Zhou QG, Cheng YX, Geng YH, Wang LX, et al. Adv Funct Mater 2006;16:101;
(c) Liu J, Zhou QG, Cheng YX, Geng YH, Wang LX, Ma DG, et al. Adv Funct Mater

2006;16:957;
(d) Liu J, Shao SY, Chen L, Xie ZY, Cheng YX, Geng YH, et al. Adv Mater 2007;19:1859;
(e) Liu J, Guo X, Bu LJ, Xie ZY, Cheng YX, Geng YH, et al. Adv Funct Mater 2007;17:1917;
(f) Niu XD, Qin CJ, Zhang BH, Yang JW, Xie ZY, Cheng YX, et al. Appl Phys Lett 2007;90:203513;
(g) Liu J, Gao BX, Cheng YX, Xie ZY, Geng YH, Wang LX, et al. Macromolecules 2008;41:1162.

[20] (a) Paik KL, Baek NS, Kim HK, Lee HJ, Lee Y. Macromolecules 2002;35:6782;
(b) Lee SK, Hwang DH, Jung BJ, Cho NS, Lee J, Lee JD, et al. Adv Funct Mater 2005;15:1647;
(c) Jiang JX, Xu YH, Yang W, Guan R, Liu ZQ, Zhen HY, et al. Adv Mater 2006;18:1769;
(d) Zhen HY, Xu W, Yang W, Chen QL, Xu YH, Jiang JX, et al. Macromol Rapid Commun 2006;27:2095.

[21] (a) Chuang CY, Shih PI, Chien CH, Wu FI, Shu CF. Macromolecules 2007;40:247;
(b) Luo J, Li XZ, Hou Q, Peng JB, Yang W, Cao Y. Adv Mater 2007;19:1113;
(c) Wu FI, Yang XH, Neher D, Dodda R, Tseng YH, Shu CF. Adv Funct Mater 2007;17:1085;
(d) Mei CY, Ding JQ, Yao B, Cheng YX, Xie ZY, Geng YH, et al. J Polym Sci Polym Chem 2007;45:1746;
(e) Wu FI, Shih PI, Tseng YH, Shu CF, Tung YL, Chi Y. J Mater Chem 2007;17:167.

[22] (a) Park MJ, Lee J, Park JH, Lee SK, Lee JI, Chu HY, et al. Macromolecules 2008;41:3063;
(b) Park MJ, Lee J, Jung IH, Park JH, Hwang DH, Shim HK. Macromolecules 2008;41:9643;
(c) Liu J, Cheng YX, Xie ZY, Geng YH, Wang LX, Jing XB, et al. Adv Mater 2008;20:1357;
(d) Zhang K, Chen Z, Yang CL, Tao YT, Zou Y, Qin JG, et al. J Mater Chem 2008;18:291.

[23] (a) Abbel R, Grenier C, Pouderoijen MJ, Stouwdam JW, Leclère PELG, Sijbesma RP, et al. J Am Chem Soc 2009;131:833;
(b) Guo X, Qin CJ, Cheng YX, Xie ZY, Geng YH, Jing XB, et al. Adv Mater 2009;21:3682.

[24] (a) Pourtois G, Beljonne D, Moucheron C, Schumm S, Mesmaeker AKD, Lazzaroni R, et al. J Am Chem Soc 2004;126:683;
(b) Fantacci S, De Angelis F, Wang J, Bernhard S, Selloni A. J Am Chem Soc 2004;126:9715;
(c) Ciofini I, Lainé PP, Bedioui F, Adamo C. J Am Chem Soc 2004;126:10763;
(d) Abedin-Siddique Z, Ohno T, Nozaki K. Inorg Chem 2004;43:663;
(e) Zou X, Ren AM, Feng JK. Polymer 2004;45:7747.

[25] (a) Jorge FE, Autschbach J, Ziegler T. J Am Chem Soc 2005;127:975;
(b) Browne WR, O'Boyle NM, Henry W, Guckian AL, Horn S, Fett T, et al. J Am Chem Soc 2005;127:1229;
(c) Nazeeruddin MK, Angelis FD, Fantacci S, Selloni A, Viscardi G, Liska P, et al. J Am Chem Soc 2005;127:16835;
(d) Horsman GP, Jirasek A, Vaillancourt FH, Barbosa CJ, Jarzecki AA, Xu C, et al. J Am Chem Soc 2005;127:16882;
(e) Mack J, Asano Y, Kobayashi N, Stillman MJ. J Am Chem Soc 2005;127:17697;
(f) Petit L, Maldivi P, Adamo C. J Chem Theory Comput 2005;1:953;
(g) Rosa A, Ricciardi G, Baerends EJ, Zimin M, Rodgers MAJ, Matsumoto S, et al. Inorg Chem 2005;44:6609;
(h) Gahungu G, Zhang JP. J Phys Chem B 2005;109:17762;
(i) Geskin VM, Grozema FC, Siebbeles LDA, Beljonne D, Brédas JL, Cornil J. J Phys Chem B 2005;109:20237;
(j) Lukeš V, Aquino A, Lischka H. J Phys Chem A 2005;109:10232;
(k) Yang L, Feng JK, Liao Y, Ren AM. Polymer 2005;46:9955;
(l) Yang L, Feng JK, Ren AM. Polymer 2005;46:10970.

[26] (a) Jacquemin D, Preat J, Wathelet V, Fontaine M, Perpète EA. J Am Chem Soc 2006;128:2072;
(b) Barolo C, Nazeeruddin MK, Fantacci S, Censo DD, Comte P, Liska P, et al. Inorg Chem 2006;45:4642;
(c) Ghosh S, Chaitanya GK, Bhanuprakash K, Nazeeruddin MK, Grätzel M, Reddy PY. Inorg Chem 2006;45:7600;
(d) Lam WH, Cheng ECC, Yam VWW. Inorg Chem 2006;45:9434;
(e) De Angelis F, Fantacci S, Sgamellotti A, Cariati E, Ugo R, Ford PC. Inorg Chem 2006;45:10576;
(f) Liang WZ, Zhao Y, Sun J, Song J, Hu SL, Yang JL. J Phys Chem B 2006;110:9908;
(g) Gahungu G, Zhang B, Zhang JP. J Phys Chem B 2006;110:16852;
(h) Fabiano E, Sala FD, Barbarella G, Lattante S, Anni M, Sotgiu G, et al. J Phys Chem B 2006;110:18651;
(i) Oliva MM, Casado J, Hennrich G, López Navarrete JT. J Phys Chem B 2006;110:19198;
(j) Lundqvist MJ, Nilsing M, Lunell S, Akermark B, Persson P. J Phys Chem B 2006;110:20513;
(k) Fernádez EJ, Laguna A, Lépez-de-Luzuriaga JM, Monge M, Montiel M, Olmos ME, et al. Organometallics 2006;25:3639;
(l) Yang L, Feng JK, Liao Y, Ren AM. Polymer 2006;47:774;
(m) Yang L, Feng JK, Ren AM, Sun JZ. Polymer 2006;47:1397;
(n) Yang L, Feng JK, Ren AM, Sun CC. Polymer 2006;47:3229;
(o) Ocampo C, Casanovas J, Liesa F, Alemán C. Polymer 2006;47:3257;
(p) Costanzo F, Tonelli D, Scalmani G, Cornil J. Polymer 2006;47:6692.

[27] (a) Avilov I, Minoofar P, Cornil J, Cola LD. J Am Chem Soc 2007;129:8247;
(b) Köse ME, Mitchell WJ, Kopidakis N, Chang CH, Shaheen SE, Kim K, et al. J Am Chem Soc 2007;129:14257;
(c) Medina BM, Vooren AV, Brocorens P, Gierschner J, Shkunov M, Heeney M, et al. Chem Mater 2007;19:4949;
(d) Salzner U. J Chem Theory Comput 2007;3:219;
(e) Salzner U. J Chem Theory Comput 2007;3:1143;
(f) Amicangelo JC. J Chem Theory Comput 2007;3:2198;
(g) Soldatova AV, Kim J, Peng X, Rosa A, Ricciardi G, Kenney ME, et al. Inorg Chem 2007;46:2080;
(h) Petsalakis ID, Tagmatarchis N, Theodorakopoulos G. J Phys Chem C 2007;111:14139;
(i) Oliva MM, Casado J, NavarreteGunther JTL, Delgado HCR, Orduna J. J Phys Chem C 2007;111:18778;
(j) Zhang YX, Cai X, Zhou Y, Zhang XX, Xu H, Liu ZQ, et al. J Phys Chem A 2007;111:392;
(k) Hu B, Gahungu G, Zhang JP. J Phys Chem A 2007;111:4965;
(l) Choe YK, Nagase S, Nishimoto K. J Comput Chem 2007;28:727;
(m) Chidthong R, Hannongbua S, Aquino AJA, Wolschann P, Lischka H. J Comput Chem 2007;28:1735;
(n) Zhang GL, Zhang H, Sun M, Liu YH, Pang XH, Yu XY, et al. J Comput Chem 2007;28:2260;
(o) Liu T, Gao JS, Xia BH, Zhou X, Zhang HX. Polymer 2007;48:502;
(p) Yang L, Feng JK, Wong WY, Poon SY. Polymer 2007;48:6457.

[28] (a) Saito K, Nakao Y, Sakaki S. Inorg Chem 2008;47:4329;
(b) Alary F, Boggio-Pasqua M, Heully JL, Marsden CJ, Vicendo P. Inorg Chem 2008;47:5259;
(c) Lukeš V, Matuszná K, Rapta P, Šolc R, Dunsch L, Aquino AJA, et al. J Phys Chem C 2008;112:3949;
(d) Piacenza M, Sala FD, Farinola GM, Martinelli C, Gigli G. J Phys Chem B 2008;112:2996;
(e) Gu X, Fei T, Zhang HY, Xu H, Yang B, Ma YG, et al. J Phys Chem A 2008;112:8387;
(f) Okur S, Salzner U. J Phys Chem A 2008;112:11842;
(g) Cheng CW, Lee YP, Witek HA. J Phys Chem A 2008;112:11998;
(h) Liao Y, Ma J. Organometallics 2008;27:4636.

[29] (a) Pan QJ, Zhou X, Guo YR, Fu HG, Zhang HX. Inorg Chem 2009;48:2844;
(b) Hung YC, Jiang JC, Chao CY, Su WF, Lin ST. J Phys Chem B 2009;113:8268;
(c) Minaev B, Minaeva V, Ågren H. J Phys Chem A 2009;113:726;
(d) Li W, Yang F, Wang ZD, Hu JM, Ma JS. J Phys Chem A 2009;113:3375;
(e) Jacquemin D, Perpète EA, Laurent AD, Assfeld X, Adamo C. Phys Chem Chem Phys 2009;11:1258.

[30] (a) Clark AE, Qin CY, Li ADQ. J Am Chem Soc 2007;129:7586;
(b) Belletête M, Morin JF, Leclerc M, Durocher G. J Phys Chem A 2005;109:6953;
(c) Yang GC, Su ZM, Qin CS. J Phys Chem A 2006;110:4817;
(d) Yang GC, Liao Y, Su ZM, Zhang HY, Wang Y. J Phys Chem A 2006;110:8758;
(e) Belletête M, Blouin N, Boudreault PLT, Leclerc M, Durocher G. J Phys Chem A 2006;110:13696;
(f) Yang GC, Su T, Shi SQ, Su ZM, Zhang HY, Wang Y. J Phys Chem A 2007;111:2739;
(g) Li N, Jia K, Wang S, Xia A. J Phys Chem A 2007;111:9393;
(h) Liu YL, Feng JK, Ren AM. J Phys Chem A 2008;112:3157;
(i) Ran XQ, Feng JK, Liu YL, Ren AM, Zou LY, Sun CC. J Phys Chem A 2008;112:10904;
(j) Šolc R, Lukeš V, Klein E, Griesser M, Kelterer AM. J Phys Chem A 2008;112:10931;
(k) Zou LY, Ren AM, Feng JK, Liu YL, Ran XQ, Sun CC. J Phys Chem A 2008;112:12172;
(l) Ran XQ, Feng JK, Ren AM, Li WC, Zou LY, Sun CC. J Phys Chem A 2009;113:7933;
(m) Yang SJ, Kertesz M. Macromolecules 2007;40:6740;
(n) Chen RF, Zheng C, Fan QL, Huang W. J Comput Chem 2007;28:2091;
(o) Liu YL, Feng JK, Ren AM. J Comput Chem 2007;28:2500;
(p) Yang B, Kim SK, Xu H, Park Y, Zhang HY, Gu C, et al. ChemPhysChem 2008;9:2601.

[31] (a) Justin Thomas KR, Lin JT, Velusamy M, Tao YT, Chuen CH. Adv Funct Mater 2004;14:83;
(b) Kato SI, Matsumoto T, Shigeiwa M, Gorohmaru H, Maeda S, Ishi-i T, et-al. Chem Eur J 2006;12:2303.

[32] Chen CH, Shi JM. Coord Chem Rev 1998;171:161.

[33] Van Slyke SA, Bryan PS, Lovencchio FV. US Patent 1990, 5, 150, 006.

[34] Hariharan PC, Pople JA. Mol Phys 1974;27:209.

[35] Gordon MS. Chem Phys Lett 1980;76:163.

[36] Frisch MJ, Pople JA, Binkley JS. J Chem Phys 1984;80:3265.

[37] (a) Roothan CCJ. Rev Mod Phys 1951;23:69;
(b) Pople JA, Nesbet RK. J Chem Phys 1954;22:571;
(c) McWeeny R, Dierksen G. J Chem Phys 1968;49:4852.

[38] Parr RG, Yang W. Density functional theory of atoms and molecules. Oxford: Oxford University Press; 1989.

[39] Lee C, Yang W, Parr RG. Phys Rev B 1988;37:785.

[40] Stephens PJ, Devlin FJ, Chabalowski CF, Frisch MJ. J Phys Chem 1994;98:11623.

[41] (a) Becke AD. J Chem Phys 1993;98:5648;
(b) Perdew JP. Phys Rev B 1986;33:8822.

[42] Becke AD. J Chem Phys 1992;96:2155.
[43] Becke AD. J Chem Phys 1992;97:9173.
[44] Perdew JP, Wang Y. Phys Rev B 1992;45:13244.
[45] (a) Ernzerhof M, Scuseria GE. J Chem Phys 1999;110:5029;
(b) Adamo C, Barone V. J Chem Phys 1999;110:6158.
[46] Stratmann RE, Scuseria GE, Frisch MJ. J Chem Phys 1998;109:8218.
[47] Bauernschmitt R, Ahlrichs R. Chem Phys Lett 1996;256:454.
[48] Casida ME, Jamorski C, Casida KC, Salahub DR. J Chem Phys 1998;108:4439.
[49] (a) Foresman JB, Head-Gordon M, Pople JA, Frisch MJ. J Phys Chem 1992;96:135;
(b) Foresman JB, Schlegel HB. In: Gausto R, Hollas JM, editors. Recent experimental and computational advances in molecular spectroscopy, vol. 406. Dordrecht, The Netherlands: Kluwer Academic; 1993. p. 11;
(c) Halls MD, Schlegel HB. Chem Mater 2001;13:2632;
(d) Tirapattur S, Belletête M, Leclerc M, Durocher G. Theochem 2003;625:141;
(e) Yang L, Feng JK, Ren AM. J Comput Chem 2005;26:969.
[50] (a) Miertuš S, Scrocco E, Tomasi J. Chem Phys 1981;55:117;
(b) Miertuš S, Tomasi J. Chem Phys 1982;65:239;
(c) Cossi M, Barone V, Camni R, Tomasi J. Chem Phys Lett 1996;255:327.
[51] Wang JF, Feng JK, Ren AM, Liu XD, Ma YG, Lu P, et-al. Macromolecules 2004;37:3451.
[52] Frisch MJ, Trucks GW, Schlegel HB, Scuseria GE, Robb MA, Cheeseman JR, et al. Gaussian 03, revision B.03. Pittsburgh, PA: Gaussian, Inc.; 2003.
[53] Jo J, Chi C, Höger S, Wegner G, Yoon DY. Chem Eur J 2004;10:2681.
[54] Gruhn NE, da Silva Filho DA, Bill TG, Malagoli M, Coropceanu V, Kahn A, et al. J Am Chem Soc 2002;124:7918.
[55] Malagoli M, Brédas JL. Chem Phys Lett 2000;327:13.
[56] Lin BC, Cheng CP, You ZQ, Hsu CP. J Am Chem Soc 2005;127:66.